JOURNAL OF NEUROTRAUMA 36:1008–1017 (April 1, 2019)

DOI: 10.1089/neu.2018.5844

Cortical Spreading Depression Denotes Concussion Injury

James Bouley,[1] David Y. Chung,[2,3] Cenk Ayata,[2,3] Robert H. Brown, Jr,[1] and Nils Henninger[1,4]

Abstract

Cortical spreading depression (CSD) has been described after moderate-to-severe traumatic brain injury (TBI). It is uncertain, however, whether CSD occurs after mild, concussive TBI and whether it relates to brain pathology and functional outcome. Male C57BL6/J mice ($n = 62$) were subjected to closed head TBI with a 25 g weight ($n = 11$), 50 g weight ($n = 45$), or sham injury ($n = 6$). Laser Doppler flowmetry and optical intrinsic signal imaging were used to determine cerebral blood flow dynamics after concussive CSD. Functional deficits were assessed at baseline, 2 h, 24 h, and 48 h. TUNEL and Prussian blue staining were used to determine cell death and presence of cerebral microbleeds at 48 h. No CSD was observed in mice subjected to a 25 g weight drop whereas 58.9% of mice subjected to a 50 g weight drop developed a CSD. Mice with concussive CSD displayed significantly greater numbers of apoptotic cell profiles in the ipsilesional hemisphere compared with mice without a CSD that underwent the same 50 g weight drop paradigm ($p < 0.05$, each). All investigated animals had at least one cerebral microbleed (range 1 to 24). Compared with mice without a CSD, mice with a CSD had significantly more microbleeds in the traumatized hemisphere ($p < 0.05$, each) and showed impaired functional recovery ($p < 0.05$). Incidence of CSD after mild TBI depended on impact severity and was associated with histological and behavioral outcomes. These observations indicate that concussive CSD may serve as viable marker for concussion severity and provide novel avenues for outcome prediction and therapeutic decision making.

Keywords: cerebral blood flow; cerebral microbleed; concussion; cortical spreading depolarization; traumatic brain injury

Introduction

Closed head injury constitutes the most common traumatic brain injury (TBI) mechanism and approximately 70–90% of all TBIs are considered mild.[1,2] Yet, despite the seemingly mild injury severity, a significant subset of affected patients have residual deficits that adversely affect their ability to perform daily activities and to return to work.[3–6] Based on consensus, concussion injury has been defined broadly as a complex pathophysiological process that affects the brain after mild TBI and is associated with a range of physical signs, cognitive impairment, neurobehavioral features, and sleep disturbances.[7] Despite the devastating impact and high prevalence of concussive TBI, however, the mechanisms that drive pathology as well as markers that can help identify concussion injury remain to be clarified.[7]

Reliable identification of concussion injury is an important goal to assist rendering decisions regarding return to play, school, and work, as well as to counsel affected subjects, tailor management, and determine the risk for brain injury and neurological sequelae.[7,8] In this respect, cortical spreading depression (CSD) after TBI could be a particularly promising biomarker for the presence of concussion-related brain injury. For several decades, it has been speculated whether spreading depressions occur after concussive human TBI.[8–11] It has been described that moderate-to-severe TBI with associated overt structural brain damage can trigger CSDs.[12–15] Although previous experimental studies using animal TBI models suggested the presence of concussive CSD, results are difficult to interpret because the majority of investigated animals displayed overt cortical contusions and subarachnoid hemorrhage.[16,17] Thus, the occurrence of CSDs and their association with concussion severity and outcome remain undefined.[9,10]

To elucidate this issue, we used a mouse model that mimics the most common form of concussive TBI[18] to determine the incidence of CSD as well as to examine the association of CSD with markers of cerebral tissue integrity and functional outcome. To enable noninvasive assessment of CSD through the intact skull in our closed-head TBI paradigm, we determined concussive CSD based on the characteristic cerebral blood flow (CBF) dynamics that represent accepted surrogate markers for CSDs as previously confirmed by us and others using electrophysiological recordings.[18–22] Our main hypothesis was that CSDs are common after concussive TBI and relate to concussion severity.

Methods

Ethical approval

All procedures were approved by the University of Massachusetts Medical School Institutional Animal Care and Use Committee.

[1]Department of Neurology, University of Massachusetts Medical School, Worcester, Massachusetts.
Departments of [2]Neurology and [3]Radiology, Massachusetts General Hospital, Boston, Massachusetts.
[4]Department of Psychiatry, University of Massachusetts Medical School, Worcester, Massachusetts.

Experimental design and animals

This pre-clinical study was designed to characterize the incidence of concussive CSD and its relation to histological and functional outcome. To this end, spontaneously breathing male C57BL6/J mice ($n=62$, Jackson Laboratories) weighing 27.5 ± 6.0 g (age 8–12 weeks) underwent closed head TBI with a 50 g weight ($n=45$), 25 g weight ($n=11$), or sham injury ($n=6$). The 50 g TBI paradigm was chosen based on our previous observations that this closed-head injury produces a mild, concussive TBI as based on the mild severity of neurological deficits, presence of traumatic axonal injury, but absent macroscopic brain injury consistent with human concussion.[7,18,23] We included a sham group to control for potential non-impact related confounders such as anesthesia and analgesia and a milder 25 g TBI paradigm to determine whether the impact severity is an important determinant for CSD.

We excluded two 25 g mice and three 50 g mice because the Laser Doppler flowmetry (LDF) probe dislodged after impact. LDF was used to assess the temporal evolution of the relative regional CBF in all included mice ($n=57$). Seven mice that underwent 50 g TBI had a femoral artery catheter placed to assess continuously the mean arterial blood pressure (MAP) concurrently with the CBF. These animals were sacrificed immediately after the completion of CBF measurements and were not included in the neurological and histological analyses. In addition, we assessed CBF over the contralesional, nontraumatized hemisphere in six mice that underwent 50 g TBI. These mice were also excluded from behavioral and histological analyses.

Neurobehavioral deficits were determined from acute to subacute time points utilizing the Neurological Severity Score (NSS), which has been validated to determine neurological sequelae in the used closed head mouse TBI model.[18] TUNEL staining was conducted to determine histological damage after TBI in a subset of mice that underwent sham injury ($n=6$) and 50 g TBI (n = 18). Prussian blue staining was obtained from a subset of mice that underwent 25 g TBI ($n=6$) and 50 g TBI ($n=12$).

Finally, we conducted exploratory cortical optical intrinsic signal (COIS) imaging in a subset of mice for qualitative assessment of the temporospatial dynamics of post-concussive CBF ($n=6$ for 25 g TBI; $n=5$ for 50 g TBI). Supplementary Figure 1 (see online supplementary material at ftp.liebertpub.com) summarizes the study design. All analyses were conducted by investigators masked to the experimental group. This article was prepared in adherence to the ARRIVE guidelines.

Anesthesia, analgesia, and TBI induction

Animals were anesthetized with isoflurane (5% for induction, 2% for surgical procedure, 1.5% for maintenance) in room air. Anesthesia was discontinued immediately before TBI and sham injury. Body temperature was monitored continuously with a rectal probe and maintained at 37.0 ± 0.5°C. To alleviate pain, animals received 0.05 mg/kg subcutaneous buprenorphine (Patterson Veterinary, Devens, MA) 30 min before the end of anesthesia and every 6 h afterward for 24 h. In addition, each animal received 5 mg/kg subcutaneous carprofen (Patterson Veterinary, Devens, MA) at the end of the anesthesia.

Closed head TBI was produced using a weight drop device as described previously in detail.[18] Briefly, the skull was exposed to allow for visualization of the sutures as landmarks for consistent impact relative to bregma (-2.5 mm in rostrocaudal and 2.5 mm lateral distance). Anesthesia was discontinued, and the animal was positioned on a 6.4 mm thick ethylene propylene diene monomer rubber surface (60 durometer hardness) with the head placed under the weight drop device. A weight (25 g or 50 g) was dropped freely 15 cm to strike a cylindrical polyacetal transducer rod (Delrin,© tip-diameter 2 mm, 17.4 g) that was placed with its tip directly on the mouse's skull under the tip at an angle of 90 degrees. Holding the transducer rod with one hand immediately after the initial impact prevented rebound impact. After TBI, skulls were examined for potential fracture and the wound closed with interrupted sutures. Sham animals were anesthetized, surgically prepared, and placed under the impact device, but were not subjected to injury.

CBF

The CBF was measured in animals using a PR407-1 straight needle LDF-probe (Perimed, Järfälla, Stockholm, Sweden) connected to a standard laser Doppler monitor (PF5010 LDPM Unit and PF5001 main unit, Perimed, Järfälla, Stockholm, Sweden). The probe was placed either over the ipsilateral traumatized ($n=45$), contralateral nontraumatized ($n=6$), or ipsilateral sham operated ($n=6$) hemisphere (approximately 3 mm posterior, 6 mm lateral, and 1 mm ventral to the bregma) on the intact lateral aspect of the skull to assess CBF.[18] A stable baseline was established and recorded for 15 min, TBI was induced, anesthesia resumed after return of regular spontaneous breathing, and CBF continuously assessed for up to 90 min. For analysis, values were averaged across 5 sec epochs from baseline to 10 min after TBI and then across 1 min epochs at designated time points afterward. In addition, we calculated the area under the curve (AUC) of the CBF measured during the first 60 min of observation. All CBF data were normalized to baseline for statistical comparisons.

COIS imaging

To characterize the temporospatial hemodyamics after concussive TBI, we conducted exploratory COIS imaging based on the cortical light reflectance through the intact skull. Details regarding the principle underlying COIS and its use for the detection of CSD in mice have been described previously.[24] In brief, after midline incision and scalp reflection, the intact skull overlying both hemispheres was covered with a thin layer of mineral oil to prevent drying and enhance transparency. Images were obtained continuously every 2 sec from pre-TBI to 30 min post-TBI using a 3.1 megapixel microscope digital camera (Model #300MU-CK, AmScope, Irvine, CA). Raw images ($10\times$; 2048×1536 resolution) were converted off-line to inverted gray scale (arbitrary units) and by subtracting each image from the subsequent image to highlight temporal changes using Matlab (version R2016a, MathWorks, Natick, MA).

Neurologic evaluation

Presence of seizure activity was evaluated clinically (facial twitching as well as tail, forelimb, and hindlimb tonic-clonic or tonic movements) as described previously.[18] Because all seizures occurred while animals were still unconscious, no attempt was undertaken to grade seizure severity according to previously developed grading scales as these are partially based on loss of posture in previously conscious animals.[18,25]

Sternal recumbency was measured as the time (s) from TBI/sham injury to righting from a supine to prone position after discontinuation of anesthesia.

The NSS was assessed before TBI as well as at 2 h, 24 h, and 48 h post-operatively as described previously in detail.[18] Briefly, the NSS consists of 10 individual clinical parameters, including tasks on motor function, alertness, and physiological behavior, and examines sensorimotor integration scored on a scale from 0 (no deficit) to 10 (maximal deficit), whereby scores from three to four indicate mild TBI.[18]

Immunohistochemistry

Mice were perfused under isoflurane anesthesia through the ascending aorta with 50 mL saline and then with ice cold phosphate-buffered 4% paraformaldehyde (PFA) for 10 min. Brains were removed from the cranium, post-fixed overnight in the same fixative,

and then stored in 0.4% PFA at 4°C until further processing. Before paraffin embedding, brains were coronally pre-sectioned using a brain matrix. Histological paraffin sections, 10-μm thick, were obtained from a slice below the impact site and evaluated with immunohistochemistry. All histological analyses were performed by an investigator masked to the animal group (N.H.).

To assess cell death, the *in situ* Cell Death Detection Kit (Sigma-Aldrich, Billerica, MA) was used following the manufacturer's instructions. Samples were imaged at 40× magnification to quantify the number of terminal deoxynucleotidyl transferase-dUTP nick end labeling (TUNEL)/4',6-diamidino-2-phenylindole (DAPI) co-stained cells. To this end, all TUNEL/DAPI co-stained cells were systematically counted in the entire coronal section using nonoverlapping fields of view (FOV). Counts were conducted in two adjacent sections (100 μm apart) obtained at the level of bregma and averaged for both sections to provide the final count. Cells were counted separately for the corpus callosum, caudate putamen, and the cerebral cortex. Note that for presentation purpose, image contrast and brightness of the histological figures was enhanced by using Photoshop's nonlinear curve function across the entire image.

Cerebral microbleed detection

Sections were stained for Prussian blue reaction using an Iron Stain Kit (# HT20, Sigma-Aldrich, St Louis, MO), following the manufacturer's instructions. In brief, slides were deparaffinized and hydrated to deionized water, immersed in a freshly prepared solution of equal parts 5% potassium ferrocyanide and 5% hydrochloric acid for 10 min, rinsed with deionized water, immersed in 2% pararosaniline solution for 5 min, rinsed with deionized water, and then rapidly dehydrated and coverslipped.

To assess for microhemorrhages, samples were imaged at 40× magnification and all Prussian blue positive profiles systematically counted separately for the entire left (nontraumatized) and right (traumatized) coronal section using nonoverlapping FOVs. Counts were conducted in one section obtained approximately at 0.25 mm and –0.75 from bregma, respectively. To describe the distribution of cerebral microbleeds within each hemisphere, we conceptually divided each coronal hemisection into three regions of interest: (1) dorsal, (2) lateral, and (3) deep (see Fig. 5C). The number of Prussian blue positive profiles per section and their approximate location within each section was recorded for each mouse. In addition, we recorded the presence of microbleeds within the subarachnoid space; however, these were not counted toward the number of Prussian blue profiles. Images of positively stained sections were taken using an Olympus BX53 microscope and Soft-Imaging System with Olympus Cell Sens software version 1.18 (Olympus, Waltham, MA).

Statistical analysis

Unless otherwise stated, continuous variables are reported as mean ± standard deviation, and categorical variables are reported as proportions. Normality of data was examined using the Shapiro-Wilk test. Between-group comparisons for continuous (body weight, CBF, blood pressure, cell counts, sternal recumbency) and ordinal (relative and absolute composite NSS) variables were made with unpaired *t* test, paired *t* test, Mann-Whitney *U* test, Wilcoxon signed-rank test, Kruskal Wallis with *post hoc* Dunn method, analysis of variance (ANOVA) on ranks, two-way ANOVA, two-way repeated measures ANOVA (two-way RM ANOVA), and two-way RM ANOVA on Ranks, as appropriate. The presence of subarachnoid microbleeds was compared using the Fisher exact test. Spearman rank correlation was used to assess the association between post-traumatic CBF and the neurological deficit severity. Two-sided significance tests were used throughout, and a two-sided $p < 0.05$ was considered statistically significant. All statistical analyses were performed using SigmaPlot 12.5 (Systat Software, Inc., Germany) or IBM® SPSS® Statistics 22 (IBM®-Armonk, NY).

Results

Cerebral hemodynamics after concussive cortical spreading depression

Figure 1 depicts the CBF response in the wake of a CSD as assessed by LDF in relation to the MAP ($n = 7$ mice). In this experiment, we noted the characteristic vasomotor components (I–IV) that accompany a CSD similar to those elicited in the same mouse strain and under the same anesthetic regimen (for details, see Fig. 1).[21] There was no significant change in the systemic blood pressure before and during the CSD-related CBF alterations ($F = 1.48$, overall test statistics $p = 0.08$).

Impact severity of mild, concussive TBI relates to incidence of CSD and functional deficit severity

Figure 2A summarizes the temporal evolution of CBF observed in mice that underwent sham operation, 25 g TBI, and 50 g TBI during

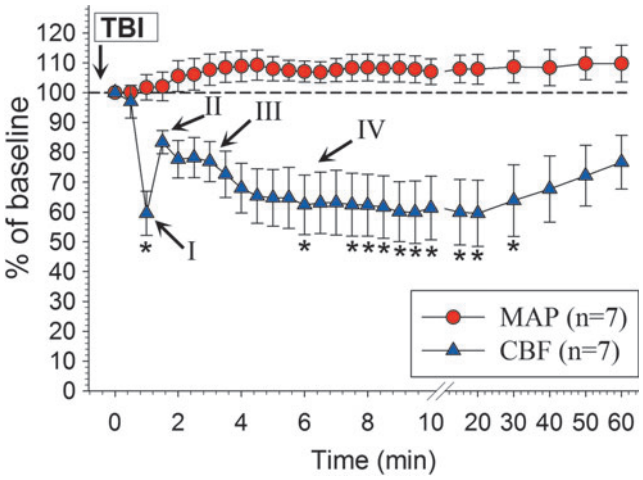

FIG. 1. Absent association between the mean arterial blood pressure (MAP) and cerebral blood flow (CBF) during the first 60 min after traumatic brain injury (TBI). There was no significant change in the MAP during the cortical spreading depression (CSD)-related CBF dynamics ($F = 1.48$, $p = 0.08$; one-way RM analysis of variance [ANOVA]) of mice that underwent 50 g TBI ($n = 7$). Roman numerals indicate the characteristic vasomotor components observed in the wake of a CSD elicited in the same mouse strain and under the same anesthetic regimen (compare also with Fig. 3) that have been described previously in detail by Ayata and Lauritzen (2015).[21] Briefly, initial vasoconstriction leads to pronounced hypoperfusion that decreases the CBF for 5–30 sec (component I: initial hypoperfusion/constriction). This is followed by pial artery dilatation resulting in augmented hyperemia with a CBF increase that usually peaks at 1–2 min (component II: peak hyperemia/dilatation). After this hyperemia peak, a second smaller, late hyperemia is observed that can last several minutes (component III: late hyperemia/dilatation). Finally, vasoconstriction causes a CBF reduction by 10–40% below baseline that may persist for an hour or longer (component IV: post-CSD oligemia/constriction).[21] Data are shown relative to the time of onset of CBF decline. $^*p < 0.05$ versus baseline ($\chi^2 = 73.8$, $DF = 26$, overall test statistics $p < 0.0001$; one-way RM ANOVA on Ranks with *post hoc* Dunnett test). For clarity in the figure, data are shown as mean ± standard error of the mean. Color image is available online.

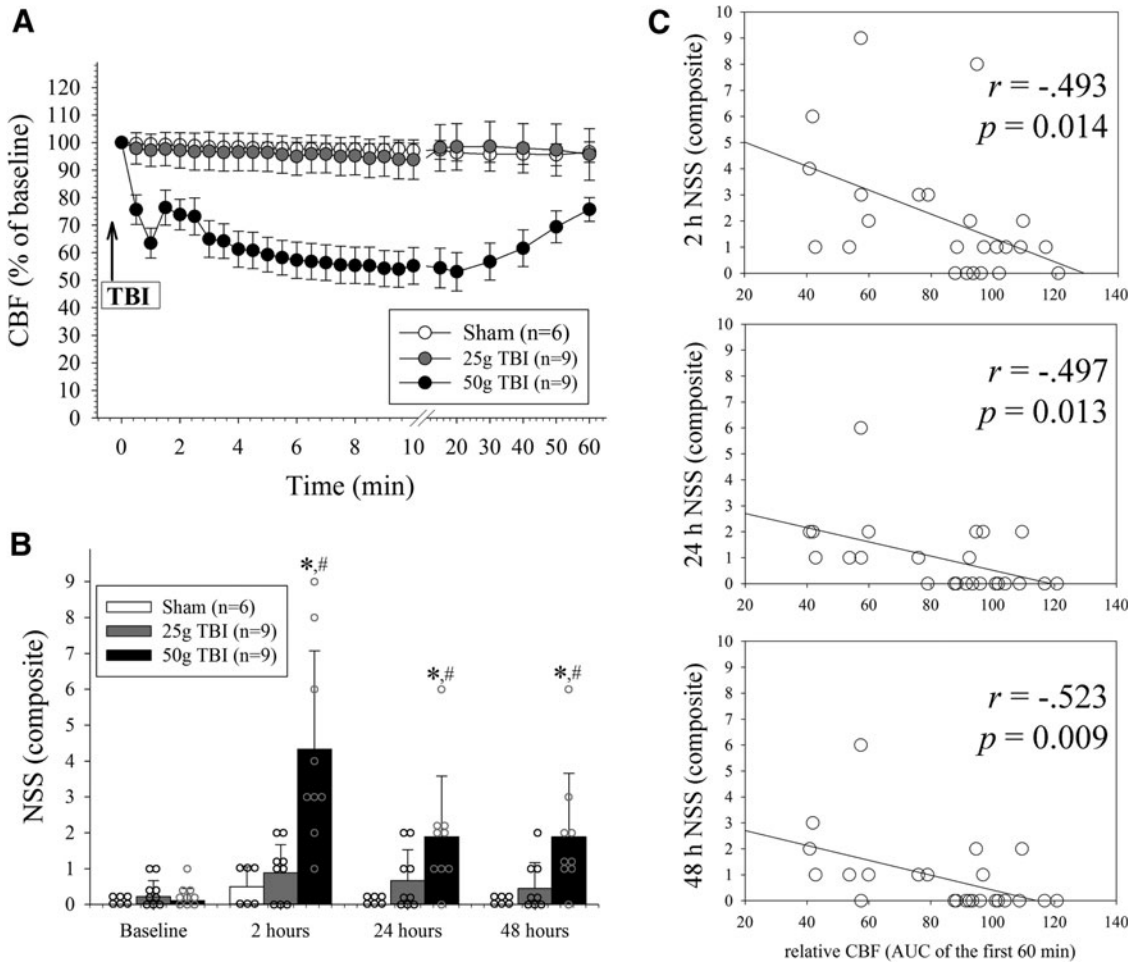

FIG. 2. Mild closed traumatic brain injury (TBI) severity relates to post-concussive cerebral hypoperfusion and functional deficit severity. (**A**) Cerebral blood flow (CBF) as assessed over the injured hemisphere. There was no significant change in the CBF in sham operated mice and animals that underwent 25 g TBI throughout the observation period, respectively ($p > 0.05$ each). Conversely, 50 g TBI was associated with a significant, progressive reduction of the CBF that persisted throughout the observation period ($p < 0.05$ vs. sham and 25 g TBI from 30 sec to 50 min; $p < 0.0001$ for group effects (DF = 2, F = 11.9), time effects (DF = 26, F = 5.0), as well as group × time interaction (DF = 52, F = 3.67); two-way RM ANOVA) For clarity in panel A, data are shown as mean ± standard error of the mean. (**B**) Composite Neurological Severity Score (NSS) increased with the impact severity ($^{*}p < 0.05$ vs. baseline; $^{\#}p < 0.05$ vs. sham; $p < 0.0001$ for group effects (DF = 2, F = 8.9) and time effects (DF = 3, F = 16.2) and $p = 0.0016$ for group × time interaction (DF = 6, F = 8.0); two-way RM ANOVA). (**C**) Significant inverse correlation between the NSS and CBF integrated over 60 min of recording ($n = 24$; Spearman rank correlation). Note, the area under the curve (AUC) was normalized to baseline and therefore exceeded 100% in animals in which the CBF increased above baseline during the post-TBI observation period.

the first 60 min after the surgical procedure. In both sham operated animals as well as mice that underwent 25 g TBI, the CBF remained stable over the 60 min observation period ($p > 0.05$ vs. baseline; two-way RM ANOVA). In contrast, there was an immediate, progressive reduction of the CBF in the ipsilateral, traumatized hemisphere consistent with a CSD ($p < 0.05$ for 30 sec to 50 min versus pre-TBI baseline). In 50 g TBI mice, the CBF reached a nadir of 53 ± 21% of baseline values by 20 min post-TBI. Thereafter, CBF gradually and partially recovered to 76 ± 13% of pre-TBI values by 60 min ($p < 0.0001$ for group and time effects, as well as group × time interaction; two-way RM ANOVA).

Figure 2B depicts the temporal evolution of the NSS observed in mice that underwent sham operation, mild 25 g TBI, and mild 50 g TBI animals during the first 48 h after operation. There was no significant change in the NSS in mice that underwent sham injury and 25 g TBI over time, respectively ($p > 0.05$; two-way RM ANOVA). Conversely, there was a significant increase in the NSS at 2 h after 50 g TBI. This observation is in line with our previous observations in the used model,[18] although the total NSS at 2 h was slightly worse in the current study, presumably because of the longer duration of anesthesia.

Across all groups, there was a significant inverse correlation between the CBF (AUC) measured during the first 60 min with the 2 h NSS, 24 h NSS, and 48 h NSS, respectively ($p < 0.05$, each; Fig. 2C).

Incidence of concussive CSD

To better understand the CSD incidence as well as to better characterize the potential association between CSD and severity of functional deficits, we conducted additional experiments in a separate cohort of mice that underwent 50 g TBI ($n = 20$). Because the overall CSD-related CBF dynamics were similar to those observed in the experiment comparing CBF across TBI severities

(compare Fig. 2A), we combined the data from all 50 g TBI mice ($n = 29$). Similar to the first experiment, a CSD developed in only 58.9% of 50 g TBI mice as determined by the characteristic CBF response (Fig. 3A–C).[21] Mice without a CSD showed a stable average CBF remaining above 80% of baseline throughout the first 90 min after TBI.

Using COIS imaging in a subset of mice, we observed a spreading concentric wave of oligemia corresponding to CSD-related CBF dynamics that was restricted to the ipsilateral, traumatized, hemisphere (Fig. 3D). Consistent with this observation, we only observed a brief CBF decline (to 75 ± 14% of baseline values at 1 min) over the contralesional, nontraumatized hemisphere in mice that underwent 50 g TBI ($n = 6$) as assessed by LDF. Afterward, the CBF in the uninjured hemisphere recovered rapidly to 90% of baseline values by 5 min and remained stable over the remaining observation period (not shown). In this experiment, mice without COIS-identified CSD had a stable ipsilesional CBF above 80% of baseline. Finally, based on the LDF and COIS imaging all CSD occurred immediately after the concussion, no mouse had more than one CSD during the observation period, and no mouse that underwent 25 g TBI had a CSD (not shown).

CSDs predict worse tissue injury

Sham animals had virtually no TUNEL positive cells (Fig. 4A). Overall, in 50 g TBI mice, there were significantly fewer apoptotic cell profiles in the contralesional (noninjured) cerebral hemisphere compared with the ipsilesional (concussed) hemisphere ($z = -1.98$, $p = 0.048$; Fig. 4B). This association was similar for all investigated regions but only reached significance for the corpus callosum ($z = 2.86$, $p = 0.003$) but not the caudate putamen ($z = 1.02$, $p = 0.32$) and cerebral cortex ($z = 1.78$, $p = 0.08$; Fig. 4C) after adjustment for multiple comparisons.

When we compared TUNEL counts in mice with ($n = 9$) versus without ($n = 9$) a concussive CSD, we found significantly more apoptotic cell profiles in the traumatized hemisphere of the former group ($p = 0.02$; Fig. 4D). This association was consistent across all investigated regions in both hemispheres: left corpus callosum

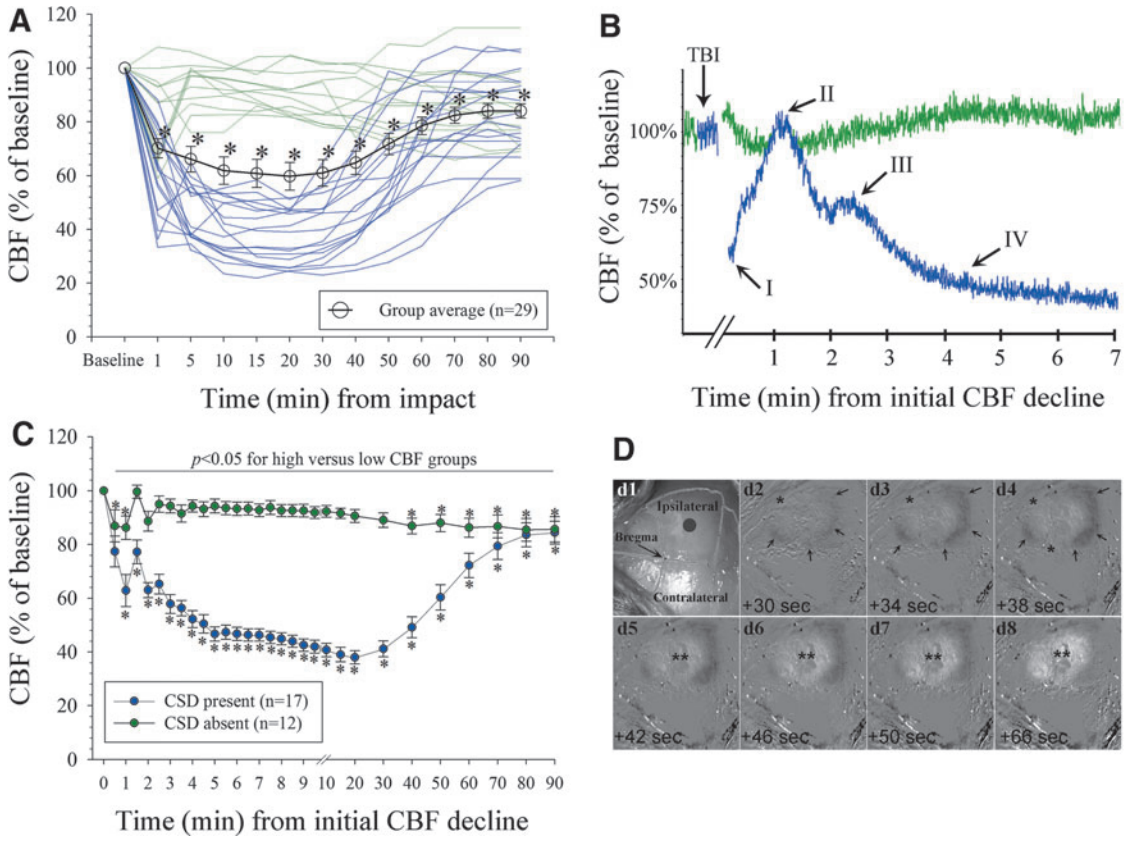

FIG. 3. Cerebral hemodynamics caused by concussive cortical spreading depression (CSD). (**A**) Group average and individual tracings of the cerebral blood flow (CBF) over the concussed hemisphere (50 g TBI) in 29 mice. Two distinct CBF responses were noted (indicated in green [''high CBF'']; CSD absent; $n = 12$] and blue [''low CBF'']; CSD present; $n = 17$]; $^*p < 0.05$ vs. baseline; overall test statistics $p < 0.0001$, $\chi^2 = 97.3$, DF = 12; one-way RM analysis of variance [ANOVA] on Ranks). For clarity in this panel, data are shown as mean ± standard error of the mean (SEM). (**B**) Representative distinct CBF profiles tracings demonstrate four vasomotor components (I–IV) indicative of a CSD in a ''low CBF'' mouse (blue; see text for details) and stable CBF in a mouse without CSD (green tracing).[21] Artifacts created by the impact were cut out for clarity in the figure (indicated by breaks). (**C**) Data from (A) shown as averaged across mice with ($n = 17$) versus without ($n = 12$) CSD and superimposed based on the initial CBF-decline ($^*p < 0.05$ vs. baseline. $p < 0.0001$ for group effects (DF = 1, F = 115.5), time effects (DF = 29, F = 20.2), and group × time interaction (DF = 29, F = 22.6), respectively; two-way RM ANOVA). For clarity in this panel, data are shown as mean ± SEM. (**D**) Representative view of the intact mouse skull with superimposed outline of the sutures (d1) after TBI (gray circle denotes impact center [not to scale]). (d2–d8) time-lapse of cortical optical intrinsic signal subtraction images (intensities inverted) shows a spreading concentric wave of oligemia (i.e., decrease in the intrinsic signal; arrows) followed by transient central hyperemia (**) consistent with established CSD-related CBF dynamics.[21] *Edge of the skull at which point the spreading wave moves ventrally out of the field of view. Color image is available online.

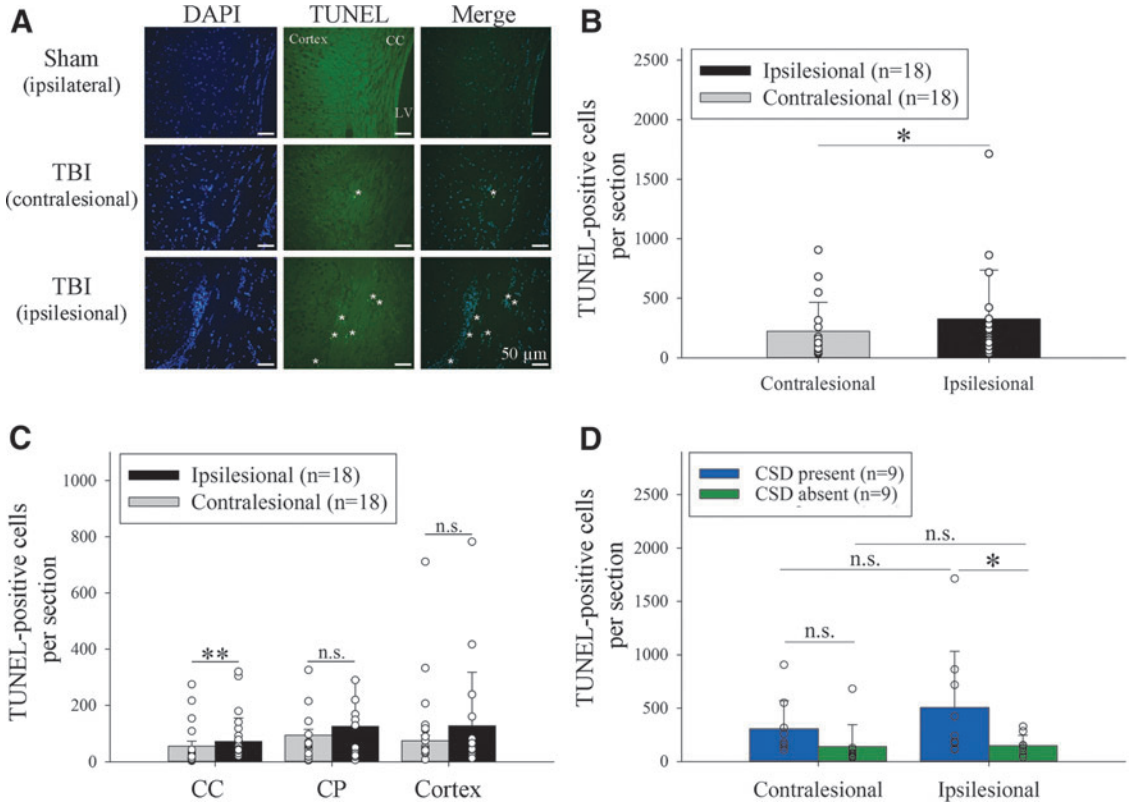

FIG. 4. Cortical spreading depression (CSD) relates to worse apoptotic cell death. **(A)** Apoptotic cell profiles at 48 h after sham operation versus 50 g TBI (40x, LV indicates lateral ventricle; asterisks indicate TUNEL/DAPI positive cells). (**B**) Significantly fewer apoptotic cell profiles in the contralesional versus ipsilesional hemisphere of 50 g TBI mice ($n = 18$; *$p < 0.05$; Wilcoxon signed-rank test). (**C**) This association was similar for all investigated regions, but only reached significance for the corpus callosum (CC; **$p < 0.01$; n.s. = not significant; CP indicates caudate putamen. (**D**) Significantly more TUNEL positive cells in the ipsilesional hemisphere of mice with ($n = 9$) versus without ($n = 9$) concussive CSD ($t = 2.4$, $p = 0.023$). Two-way analysis of variance: $p = 0.018$ for group effects (DF = 1, F = 6.2), $p = 0.34$ for side effects (DF = 1, F = 1.), and $p = 0.37$ for group × side interaction (DF = 1, F = 0.8). Color image is available online.

($z = -2.25$, $p = 0.02$); right corpus callosum ($z = -2.78$, $p < 0.01$); left caudate putamen ($z = -2.17$, $p = 0.03$), right caudate putamen ($z = -2.61$, $p = 0.01$), left cortex ($z = -2.52$, $p = 0.01$), and right cortex ($z = -2.17$, $p = 0.03$).

Finally, there was a significant correlation between the CBF measured at 5 through 50 min with the number of TUNEL positive cell profiles in ipsilesional corpus callosum, caudate putamen, and the cerebral hemisphere ($p < 0.05$, each), respectively. Similarly, there was a significant correlation between the number of apoptotic cell profiles in these areas and the CBF integrated (AUC) over 0–60 min ($p < 0.01$). Because the impact paradigm was identical for all mice, our observations indicate that CSDs predict the observed histological damage in the ipsilesional cerebral hemisphere after concussive head injury.

CSDs are associated with worse functional deficits

In light of the observed association between CSD and histological injury, we sought to determine the potential association of CSD with the functional deficit severity after TBI in our mouse model. Overall, mice that underwent 50 g TBI showed significant neurological deficits by 2 h as assessed by the NSS (*$p < 0.05$). The functional deficit severity was similar between mice with versus without a CSD at all investigated time points ($p = 0.82$ for group effects (DF = 1, F = 0.05); $p < 0.0001$ for time effects (DF = 3, F = 45.4); $p = 0.25$ for group × time interaction (DF = 3, F = 1.4). When we examined neurological recovery relative to the 2 h time point, we found that although both groups showed a similar rate of recovery ($p = 0.08$ for group × time interaction), the relative magnitude of functional recovery was less in mice with a CSD compared with those without CSDs at 24 h and 48 h, respectively ($p = 0.027$ for group effects; $p < 0.001$ for time effects; Fig. 5A).

We did not find a significant difference in the body weight between CSD groups throughout the study period ($p > 0.05$; Fig. 5B), and the recovery time from anesthesia (defined as the time to spontaneously right from a supine to prone position after discontinuation of anesthesia) was similar between mice with versus without a CSD ($p = 0.75$; Fig. 5C). This observation indicates that anesthetic effects and loss in body weight are unlikely to have contributed to the observed between-group differences in the NSS.

There was no significant correlation between the number of apoptotic cell profiles in any of the analyzed areas measured at 48 h and the composite NSS, as well as the degree of NSS recovery at any time point ($p > 0.2$, each), respectively. This suggests that the degree of apoptotic cell death, while associated with CSD, did not drive the behavior pathology observed in our model.

CSDs are associated with a greater number of cerebral microbleeds

None of the 62 mice had macroscopic evidence of a skull fracture or cerebral hemorrhage. In light of our observation that CSD

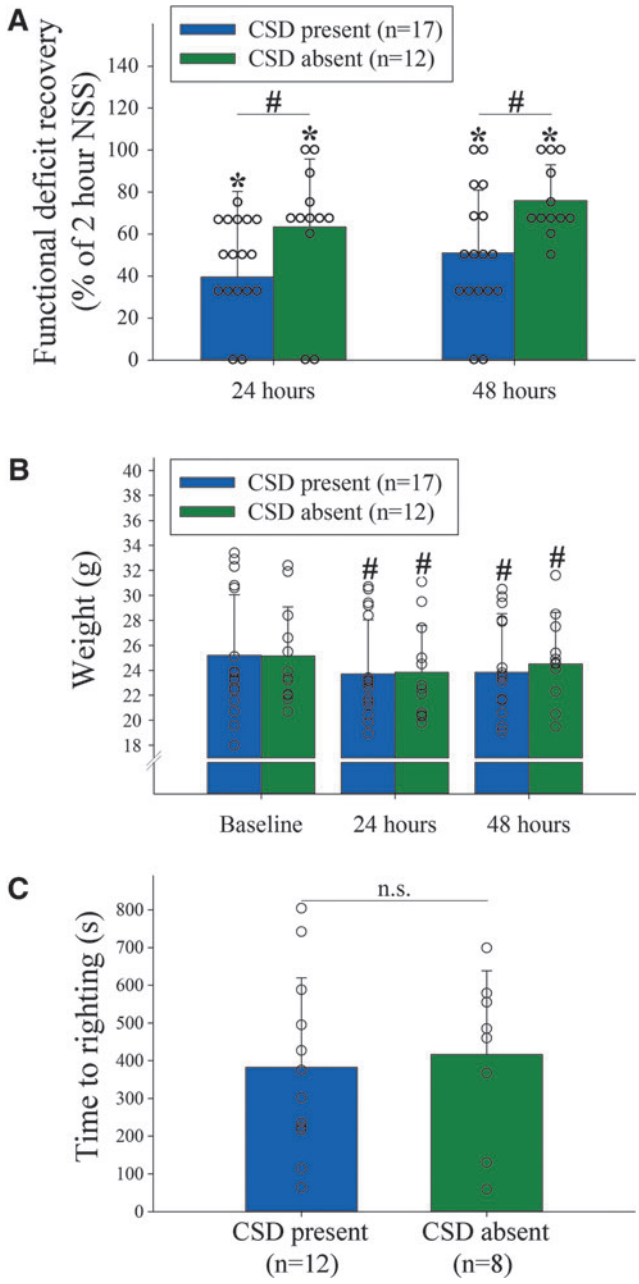

FIG. 5. Cortical spreading depression (CSD) is associated with worse functional deficit recovery. (**A**) Significantly greater relative Neurological Severity Score (NSS) recovery from the 2 h time point was observed in mice without a CSD as compared to mice with a CSD ($p=0.027$ for group effects (DF = 1, F = 5.5); $p<0.0001$ for time effects (DF = 2, F = 34.4); two-way RM analysis of variance [ANOVA]). There was no significant group × time interaction ($p=0.078$, DF = 2, F = 2.7) indicating a similar rate of recovery over time, however. (**B**) Mice with and without CSD lost weight to a similar degree over the course of the first 48 h ($p=0.93$ for group effects (DF = 1, F < 0.01); $p<0.0001$ for time effects (DF = 2, F = 55.0); $p=0.54$ for group × time interaction (DF = 2, F = 0.6); two-way RM ANOVA). (**C**) Similar time to regaining sternal recumbency after the end of anesthesia in a subset of mice with ($n=12$) versus without ($n=8$) a CSD ($p=0.75$, $t=-0.32$, DF = 18; Mann-Whitney U test). $^{\#}p<0.05$; $^{*}p<0.05$ versus baseline; n.s. = not significant. Color image is available online.

developed in only a subset of mice, we conducted exploratory analyses in 18 mice whether cerebral microbleeds, as a surrogate marker of concussion severity, related to CSD incidence. All investigated mice had at least one cerebral microbleed (range 1–24). Overall, there was no significant difference in the number of microbleeds between the more anterior (bregma +0.25 mm) and posterior (bregma –0.75 mm) coronal sections in the three subgroups (25 g TBI mice 2.7 ± 1.2 vs. 2.7 ± 2.3, $p=1.0$; 50 g TBI mice without CSD 2.8 ± 3.5 vs. 2.7 ± 2.7, $p=0.94$; 50 g TBI mice with CSD 7.5 ± 6.4 vs. 4.3 ± 4.1, $p=0.24$; paired t test). Thus, we combined the numbers from both sections for further analyses.

The number of microbleeds was similar between the nontraumatized and traumatized hemisphere of 25 g TBI mice (3.2 ± 2.4 vs. 2.2 ± 0.8, $p=0.28$) and 50 g TBI mice without CSD (3.0 ± 2.8 vs. 2.5 ± 1.9, $p=0.68$). Conversely, 50 g TBI mice with a CSD had almost twice as many microbleeds in the traumatized versus nontraumatized hemisphere (4.2 ± 4.1 vs. 7.7 ± 5.1, $p=0.005$). Further, compared with 25 g TBI and 50 g TBI mice without a CSD, mice with a CSD had significantly more microbleeds in the traumatized ($p<0.05$), but not in the nontraumatized ($p=0.79$) hemisphere (Fig. 6A).

We found that one (17%) 25 g TBI mouse, three (50%) 50 g TBI mice without CSD, and two (33%) 50 g TBI mice with CSD also had microbleeds within the subarachnoid space. There was no significant difference in the proportion of mice with subarachnoid microbleeds between the three groups ($p=0.82$, DF = 2; Fisher exact test).

The approximate location of the identified parenchymal microbleeds ($n=136$) and subarachnoid microbleeds within both investigated coronal sections are depicted in Figure 6. While microbleeds were present throughout the brain in all groups, there was nevertheless a striking clustering of microbleeds in the traumatized cortex of 50 g TBI mice with CSD (region I in Fig. 6C): the frequency of ipsilateral microbleeds within the dorsal cortex underneath the trauma site (region I) was 43% in 25 g TBI mice ($n=6/14$), 19% in 50 g TBI mice without CSD ($n=3/16$), and 61% in 50 g TBI mice with CSD ($n=28/46$; overall test statistics $p=0.009$, DF = 2, H = 9.5; ANOVA on ranks with *post hoc* Dunn's test).

Seizures

We observed no seizures among sham operated and 25 g TBI mice. Of the 50 g TBI mice used for ipsilesional CBF monitoring, $n=14$ (48%) had a clinical, self-limited seizure immediately after the impact. There was no significant difference in the presence of seizures between 50 g TBI mice with versus without a CSD (53% vs. 42%; $p=0.71$; χ^2 test). Further, there was no significant association between seizure presence and functional deficit recovery at 24 h ($p=0.43$) and 48 h ($p=0.91$), as well as the number of TUNEL positive cells in each of the investigated brain regions ($p>0.2$, each), and the number microbleeds ($p=0.76$) (all comparisons were performed by Rank sum test).

Discussion

By analyzing the immediate post-concussive CBF dynamics, we provide evidence for the frequent incidence of a concussive CSD in the absence of overt brain injury and thereby provide proof for the long-held belief that functional phenomena observed after concussive brain injury could be from CSD.[9–11,17,26,27] Importantly, we found that CSD incidence depended on concussion severity and that CSD related to the degree of post-concussive brain pathology and deficit recovery.

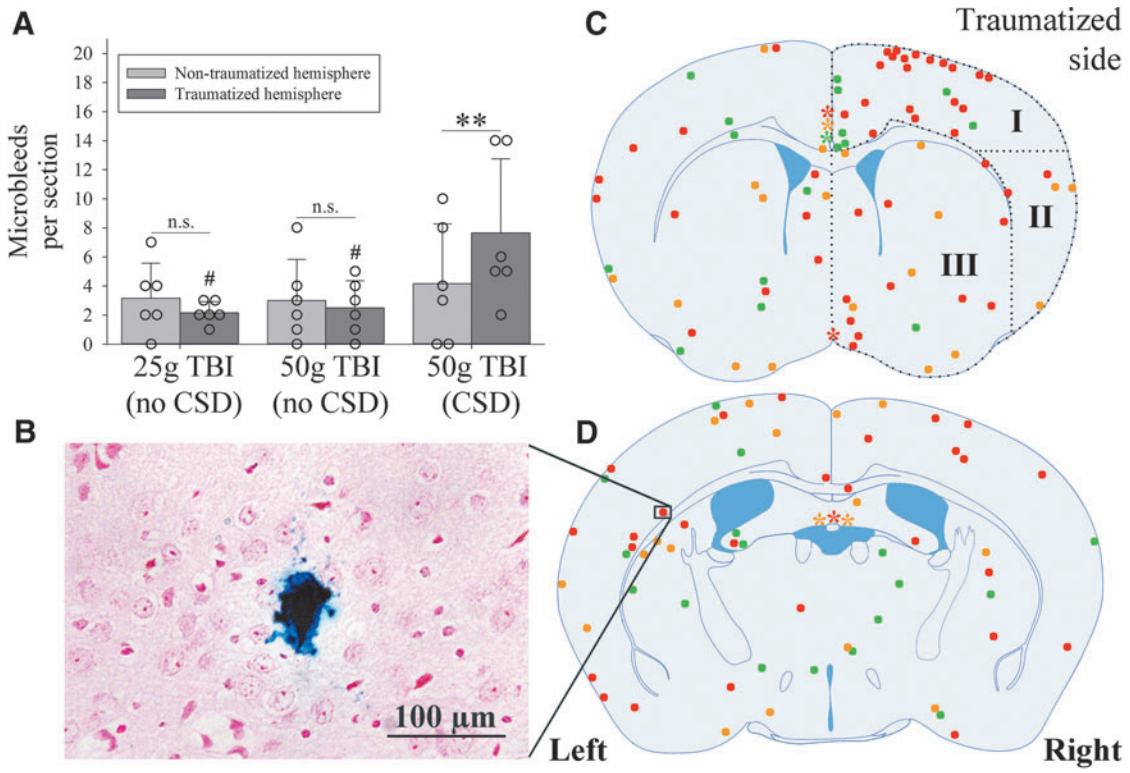

FIG. 6. Number and location of microbleeds. (**A**) 50 g TBI mice with cortical spreading depression (CSD) ($n=6$) had a significantly greater number of microbleeds in the traumatized hemisphere compared with the contralateral side (**$p=0.005$, $t=-4.9$, DF = 5; paired t test; n.s. = not significant) as well as compared with the corresponding hemisphere in 25 g TBI mice ($n=6$) and 50 g TBI mice ($n=6$) without CSD, respectively ($^{\#}p<0.05$, each; $p=0.03$ for group effects (DF = 2, F = 4.1); $p=0.53$ for side effects (DF = 1, F = 0.4); $p=0.18$ for group × side interaction (DF = 2, F = 1.8); two-way analysis of variance). (**B**) Representative microbleed as identified by Prussian blue staining (20x). (**C, D**) Approximate location of all identified cerebral microbleeds ($n=136$) in 25 g TBI mice ($n=6$; green), 50 g TBI mice without CSD ($n=6$; yellow), and 50 g TBI mice with CSD ($n=6$; red) at the level of bregma +0.25 mm (C) and −0.75 mm (D), respectively. Note that size and location of microbleeds are not to scale and only approximate because of slight differences in the actual level of the coronal section relative to bregma. Asterisks indicate the location of subarachnoid microbleeds in the interhemispheric fissure (C) and lining the dorsal third ventricle (D; color code corresponds to that of microbleeds). Black dots outline the three defined regions of interest: dorsal (I), lateral (II), and deep (III). Color image is available online.

Specifically, we found that a CSD did not develop in a mouse that underwent 25 g TBI, indicating that CSD occurrence at least in part depends on concussion severity. This is consistent with a previous experimental study that found a positive association between the impact magnitude and number of CSD in a more severe fluid percussion model.[28] More importantly, however, we found that only approximately two-thirds of mice that underwent 50 g TBI exhibited a CSD. Accordingly, impact severity alone does not sufficiently explain CSD incidence after concussive TBI. Further, we found no significant difference in the occurrence of impact seizures in mice with versus without a CSD, nor was there a significant association of seizure presence with subsequent neurological deficit recovery and histological injury. This is an important observation because seizures are an established consequence of TBI but can also both serve as trigger for CSD and can be elicited by a CSD.[29–31] Together, our results are inconsistent with the notion that impact seizures were the main cause of CSD and CSD-related histological and functional outcomes in our study.

Inter- and intra-individual variability in CSD occurrence, propagation, and duration is a well-recognized phenomenon in both animal and human studies,[13,20,32] although the reasons for this are not well understood. Known confounders such as periprocedural cardiovascular depression, differences in anesthetic depth, as well as inadvertent triggering of CSD during operation[20,21] appear highly unlikely to have contributed to variability in our study given our noninvasive surgical approach, stable blood pressure during the study period, and overall identical experimental conditions between animals. Instead, it appears more likely that unappreciated, minor differences in the trauma biomechanics between animals may have contributed to the observed variable CSD incidence. This hypothesis is supported by recent experimental observations indicating that force point loading and parenchymal shear stress foci in the cerebral cortex, rather than kinematic variables, are the key determinants of post-concussive phenomena.[8] In accord with this experimental data, recent clinical observations in athletes wearing helmets equipped with accelerometers also did not disclose a clear association between biomechanical measurements (including acceleration magnitude and impact location) with concussive symptoms.[33]

More important, we found an association of CSD with parenchymal microscopic cortical injury as well as functional recovery. It has been hypothesized that concussive TBI results in rapid neuronal membrane depolarization sufficient to trigger a CSD.[8,13,21] Accordingly, our data are consistent with the postulated link between mild TBI and concussion injury that the severity of cortical shear stress determines the degree of microvascular injury (as evidenced by significantly more cerebral microbleeds adjacent to the impact zone),

cell death, and degree of functional deficits. Once shear stress-related injury surpasses a certain threshold and depolarizes a sufficient number of neurons, a CSD is triggered.[34]

In our model, approximately 3 mm^2 of brain cortex is impacted. Given a cortical thickness of 1 mm,[35,36] a cortical volume of approximately 3 mm^3 is directly impacted. In addition, impact-related skull deformation and strain-related energy propagation likely resulted in additional involvement of cortical tissues beyond the actual impact zone[37,38] leading to involvement of more than 1 mm^3 cortex, the minimally required tissue volume to trigger a CSD *in vivo*.[34] This strongly supports the notion that CSD may, therefore, serve as a candidate marker for concussion severity and risk for subsequent neurological sequelae. If validated, our data indicate that assessment for CSD—e.g., by noninvasive transcranial CBF assessment—could aid clinical risk assessment and decision making.

Although our data show that CSDs relate to concussion severity and related phenomena, our study does not establish causality between CSD and assessed outcome measures. Therefore, it remains presently uncertain whether CSD are a consequence, epiphenomenon, or driver of observed pathology and worse functional outcomes in our study. For example, in the unperturbed brain, CSDs are fully reversible without any signs of cellular damage in otherwise metabolically intact tissue.[21,39] Although adverse hemodynamic responses to CSD have been demonstrated in human severe TBI including inverse neurovascular coupling and aggravated cerebral ischemic conditions,[21,40] it is unclear whether concussive CSDs, which occur in the absence of major tissue injury and cerebral hypoperfusion, cause metabolic compromise to induce tissue injury.[18,21] Further, in our study, increased TUNEL positive cells were noted not only in the traumatized cortex but also in the non-traumatized cortex as well as bilaterally in the corpus callosum and caudate putamen.

Future studies are needed to define the precise role of concussive CSD and related hemodynamic responses, in causing tissue injury, including a thorough characterization of neuronal versus non-neuronal cell death, and functional outcome after mild TBI. Demonstration of an independent contribution of CSD to concussive brain injury would hold great promise for the identification of original treatment targets and the development of viable therapeutic approaches, which is an important goal because to date all therapies failed to translate from the laboratory to human TBI.[41,42]

A strength of our study rests with the utilization of a mouse model of concussive head injury as well as the noninvasive assessment of concussive CSD based on the characteristic CBF dynamics in the cortex of isoflurane-anesthetized mice that represent accepted surrogate markers for CSDs and to assess related pathophysiology.[18–21] Nevertheless, future studies seeking to provide comprehensive insight into the association of concussive CSDs with outcome may benefit from additional assessment of neuronal electrical activity, which represents the foundation of cerebral function.

Further, future studies may benefit from including cognitive and histological assays to directly determine the contribution of CSD to chronic neurodegenerative changes and cognitive deficit severity with an extended follow-up period. Further, all our investigations were conducted among male mice. Given potential sex differences with respect to CSD-susceptibility, future studies should include female mice.[43] Last, because our study represents the first detailed report on CSD in rodent closed head mild TBI, there were no data to inform valid *a priori* sample size calculations. Arguably, given the observational nature of our study, this issue does not represent a major shortcoming, and the results gained from our study are well suited to inform future study design.

Conclusion

Using a closed head mouse model of mild, concussive TBI, we provide evidence for concussive CSD and that CSD occurrence relates to impact severity as well as histological and behavioral outcomes. Our observations are of high translational relevance and could provide novel avenues for outcome prediction and therapeutic intervention both in experimental and human TBI studies.

Acknowledgments

We gratefully acknowledge expert assistance provided by Y. Liu (Morphology Core Laboratory; University of Massachusetts Medical School) for histotechnological assistance, A. Weiss for animal husbandry, K. van der Marel (Department of Radiology, University of Massachusetts Medical School) for implementation of the Matlab code to process COIS images, and K. Benoit for tireless logistical assistance and administrative support. This study was supported by institutional grants, National Institutes of Health grant NS091499 to N.H., NS055104, NS102969 to C.A., NS065743 to D.Y.C., and NS088689, FD004127, HD060848 to R.H.B. N.H. serves on the advisory board of Omniox, Inc. C.A receives support from the Fondation Leducq, the Heitman Foundation, and the Ellison Foundation. R.H.B. receives support from the Angel Fund, the ALS Association, ALSFindingaCure, the Cellucci Fund for ALS Research, Project ALS and the Pierre deBourghknect ALS Fund. R.H.B. is a co-founder of AviTx.

Portions of data presented in this article are part of the doctoral thesis of N.H.

Author Disclosure Statement

No competing financial interests exist.

References

1. Faul, M.D., Xu, L., Wald, M.M., and Coronado, V.G. (2010). Traumatic Brain Injury in the United States: Emergency Department Visits, Hospitalizations and Deaths 2002–2006. Centers for Disease Control and Prevention, National Center for Injury Prevention and Control: Atlanta.
2. Feigin, V.L., Theadom, A., Barker-Collo, S., Starkey, N.J., McPherson, K., Kahan, M., Dowell, A., Brown, P., Parag, V., Kydd, R., Jones, K., Jones, A., Ameratunga, S., and Bionic Study Group. (2013). Incidence of traumatic brain injury in New Zealand: a population-based study. Lancet Neurol. 12, 53–64.
3. McAllister, T.W., Sparling, M.B., Flashman, L.A., Guerin, S.J., Mamourian, A.C., and Saykin, A.J. (2001). Differential working memory load effects after mild traumatic brain injury. Neuroimage 14, 1004–1012.
4. Englander, J., Hall, K., Stimpson, T., and Chaffin, S. (1992). Mild traumatic brain injury in an insured population: subjective complaints and return to employment. Brain Inj. 6, 161–166.
5. Stalnacke, B.M., Elgh, E., and Sojka, P. (2007). One-year follow-up of mild traumatic brain injury: cognition, disability and life satisfaction of patients seeking consultation. J. Rehabil. Med. 39, 405–411.
6. Hoge, C.W., McGurk, D., Thomas, J.L., Cox, A.L., Engel, C.C., and Castro, C.A. (2008). Mild traumatic brain injury in U.S. Soldiers returning from Iraq. N. Engl. J. Med. 358, 453–463.
7. McCrory, P., Meeuwisse, W., Aubry, M., Cantu, B., Dvorak, J., Echemendia, R.J., Engebretsen, L., Johnston, K., Kutcher, J.S., Raftery, M., Sills, A., Schneider, K., Tator, C.H., Benson, B.W., Davis, G.A., Ellenbogen, R.G., Guskiewicz, K.M., Herring, S.A., Iverson, G., Jordan, B.D., Kissick, J., McCrea, M., McIntosh, A.S., Maddocks, D.L., Makdissi, M., Purcell, L., Putukian, M., Turner, M., Schneider, K., and Tator, C.H. (2013). Consensus statement on concussion in sport—the 4th International Conference on Concussion in Sport held in Zurich, November 2012. Clin. J. Sport Med. 23, 89–117.
8. Tagge, C.A., Fisher, A.M., Minaeva, O.V., Gaudreau-Balderrama, A., Moncaster, J.A., Zhang, X.L., Wojnarowicz, M.W., Casey, N., Lu, H., Kokiko-Cochran, O.N., Saman, S., Ericsson, M., Onos, K.D., Veksler,

R., Senatorov, V.V., Jr., Kondo, A., Zhou, X.Z., Miry, O., Vose, L.R., Gopaul, K.R., Upreti, C., Nowinski, C.J., Cantu, R.C., Alvarez, V.E., Hildebrandt, A.M., Franz, E.S., Konrad, J., Hamilton, J.A., Hua, N., Tripodis, Y., Anderson, A.T., Howell, G.R., Kaufer, D., Hall, G.F., Lu, K.P., Ransohoff, R.M., Cleveland, R.O., Kowall, N.W., Stein, T.D., Lamb, B.T., Huber, B.R., Moss, W.C., Friedman, A., Stanton, P.K., McKee, A.C., and Goldstein, L.E. (2018). Concussion, microvascular injury, and early tauopathy in young athletes after impact head injury and an impact concussion mouse model. Brain 141, 422–458.

9. Takahashi, H. and Nakazawa, S. (1980). Specific type of head injury in children. Report of 5 cases. Childs Brain 7, 124–131.
10. Oka, H., Kako, M., Matsushima, M., and Ando, K. (1977). Traumatic spreading depression syndrome. Review of a particular type of head injury in 37 patients. Brain 100, 287–298.
11. Shaw, N.A. (2002). The neurophysiology of concussion. Prog. Neurobiol. 67, 281–344.
12. Hartings, J.A., Bullock, M.R., Okonkwo, D.O., Murray, L.S., Murray, G.D., Fabricius, M., Maas, A.I., Woitzik, J., Sakowitz, O., Mathern, B., Roozenbeek, B., Lingsma, H., Dreier, J.P., Puccio, A.M., Shutter, L.A., Pahl, C., Strong, A.J., and Co-Operative Study on Brain Injury Depolarisations. (2011). Spreading depolarisations and outcome after traumatic brain injury: a prospective observational study. Lancet Neurol. 10, 1058–1064.
13. Dreier, J.P. (2011). The role of spreading depression, spreading depolarization and spreading ischemia in neurological disease. Nat. Med. 17, 439–447.
14. Hinzman, J.M., Wilson, J.A., Mazzeo, A.T., Bullock, M.R.. and Hartings, J.A. (2016). Excitotoxicity and metabolic crisis are associated with spreading depolarizations in severe traumatic brain injury patients. J. Neurotrauma 33, 1775–1783.
15. Hartings, J.A., Watanabe, T., Bullock, M.R., Okonkwo, D.O., Fabricius, M., Woitzik, J., Dreier, J.P., Puccio, A., Shutter, L.A., Pahl, C., Strong, A.J.. and Co-Operative Study on Brain Injury, D. (2011). Spreading depolarizations have prolonged direct current shifts and are associated with poor outcome in brain trauma. Brain 134, 1529–1540.
16. West, M., Parkinson, D.. and Havlicek, V. (1982). Spectral analysis of the electroencephalographic response in experimental concussion in the rat. Electroencephalogr. Clin. Neurophysiol. 53, 192–200.
17. Takahashi, H., Manaka, S., and Sano, K. (1981). Changes in extracellular potassium concentration in cortex and brain stem during the acute phase of experimental closed head injury. J. Neurosurg. 55, 708–717.
18. Henninger, N., Bouley, J., Sikoglu, E.M., An, J., Moore, C.M., King, J.A., Bowser, R., Freeman, M.R., and Brown, R.H., Jr. (2016). Attenuated traumatic axonal injury and improved functional outcome after traumatic brain injury in mice lacking Sarm1. Brain 139, 1094–1105.
19. Woitzik, J., Hecht, N., Pinczolits, A., Sandow, N., Major, S., Winkler, M.K., Weber-Carstens, S., Dohmen, C., Graf, R., Strong, A.J., Dreier, J.P., Vajkoczy, P., and COSBID Study Group. (2013). Propagation of cortical spreading depolarization in the human cortex after malignant stroke. Neurology 80, 1095–1102.
20. Kaufmann, D., Theriot, J.J., Zyuzin, J., Service, C.A., Chang, J.C., Tang, Y.T., Bogdanov, V.B., Multon, S., Schoenen, J., Ju, Y.S., and Brennan, K.C. (2016). Heterogeneous incidence and propagation of spreading depolarizations. J. Cereb. Blood Flow Metab. 271678X16659496.
21. Ayata, C. and Lauritzen, M. (2015). Spreading depression, spreading depolarizations, and the cerebral vasculature. Physiol. Rev. 95, 953–993.
22. Chung, D.Y., Sadeghian, H., Qin, T., Lule, S., Lee, H., Karakaya, F., Goins, S., Oka, F., Yaseen, M.A., Houben, T., Tolner, E.A., van den Maagdenberg, A., Whalen, M.J., Sakadzic, S., and Ayata, C. (2018). Determinants of optogenetic cortical spreading depolarizations. Cereb. Cortex. Epub ahead of print.
23. Flierl, M.A., Stahel, P.F., Beauchamp, K.M., Morgan, S.J., Smith, W.R., and Shohami, E. (2009). Mouse closed head injury model induced by a weight-drop device. Nat. Protoc. 4, 1328–1337.
24. Yuzawa, I., Sakadzic, S., Srinivasan, V.J., Shin, H.K., Eikermann-Haerter, K., Boas, D.A., and Ayata, C. (2012). Cortical spreading depression impairs oxygen delivery and metabolism in mice. J. Cereb. Blood Flow Metab. 32, 376–386.
25. Samoriski, G.M. and Applegate, C.D. (1997). Repeated generalized seizures induce time-dependent changes in the behavioral seizure response independent of continued seizure induction. J. Neurosci. 17, 5581–5590.
26. Echlin, F. (1948). Spreading depression of electrical activity in the cerebral cortex following local trauma and its possible role in concussion. Trans. Am. Neurol. Assoc. 73, 199–202.
27. Echlin, F.A. (1950). Spreading depression of electrical activity in the cerebral cortex following local trauma and its possible role in concussion. Arch. Neurol. Psychiatry 63, 830–832.
28. Rogatsky, G.G., Sonn, J., Kamenir, Y., Zarchin, N., and Mayevsky, A. (2003). Relationship between intracranial pressure and cortical spreading depression following fluid percussion brain injury in rats. J. Neurotrauma 20, 1315–1325.
29. Leao, A.A.P. (1944). Spreading depression of activity in the cerebral cortex. J Neurophysiol 7, 359–390.
30. Leao, A.A.P. (1944). Pial circulation and spreading depression of activity in the cerebral cortex. J. Neurophysiol. 7, 391–396.
31. Fabricius, M., Fuhr, S., Willumsen, L., Dreier, J.P., Bhatia, R., Boutelle, M.G., Hartings, J.A., Bullock, R., Strong, A.J., and Lauritzen, M. (2008). Association of seizures with cortical spreading depression and peri-infarct depolarisations in the acutely injured human brain. Clin. Neurophysiol. 119, 1973–1984.
32. Hansen, J.M., Baca, S.M., Vanvalkenburgh, P., and Charles, A. (2013). Distinctive anatomical and physiological features of migraine aura revealed by 18 years of recording. Brain 136, 3589–3595.
33. Rowson, S., Duma, S.M., Stemper, B.D., Shah, A., Mihalik, J.P., Harezlak, J., Riggen, L.D., Giza, C.C., DiFiori, J.P., Brooks, A., Guskiewicz, K., Campbell, D., McGinty, G., Svoboda, S.J., Cameron, K.L., Broglio, S.P., McAllister, T.W., and McCrea, M. (2018). Correlation of concussion symptom profile with head impact biomechanics: a case for individual-specific injury tolerance. J. Neurotrauma 35, 681–690.
34. Matsuura, T. and Bures, J. (1971). The minimum volume of depolarized neural tissue required for triggering cortical spreading depression in rat. Exp. Brain Res. 12, 238–249.
35. Altamura, C., Dell'Acqua, M.L., Moessner, R., Murphy, D.L., Lesch, K.P., and Persico, A.M. (2007). Altered neocortical cell density and layer thickness in serotonin transporter knockout mice: a quantitation study. Cereb. Cortex 17, 1394–1401.
36. Paxinos, G. and Franklin, K.B.J. (2013). *The Mouse Brain in Stereotaxic Coordinates.* 4th ed. Elsevier Academic Press: Amsterdam.
37. Bayly, P.V., Black, E.E., Pedersen, R.C., Leister, E.P., and Genin, G.M. (2006). In vivo imaging of rapid deformation and strain in an animal model of traumatic brain injury. J. Biomech. 39, 1086–1095.
38. Levchakov, A., Linder-Ganz, E., Raghupathi, R., Margulies, S.S., and Gefen, A. (2006). Computational studies of strain exposures in neonate and mature rat brains during closed head impact. J. Neurotrauma 23, 1570–1580.
39. Dreier, J.P. and Reiffurth, C. (2015). The stroke-migraine depolarization continuum. Neuron 86, 902–922.
40. Hinzman, J.M., Andaluz, N., Shutter, L.A., Okonkwo, D.O., Pahl, C., Strong, A.J., Dreier, J.P., and Hartings, J.A. (2014). Inverse neurovascular coupling to cortical spreading depolarizations in severe brain trauma. Brain 137, 2960–2972.
41. Kochanek, P.M., Bramlett, H., Dietrich, W.D., Dixon, C.E., Hayes, R.L., Povlishock, J., Tortella, F.C., and Wang, K.K. (2011). A novel multicenter preclinical drug screening and biomarker consortium for experimental traumatic brain injury: operation brain trauma therapy. J. Trauma 71, Suppl 1, S15–S24.
42. Kochanek, P.M., Bramlett, H.M., Shear, D.A., Dixon, C.E., Mondello, S., Dietrich, W.D., Hayes, R.L., Wang, K.K., Poloyac, S.M., Empey, P.E., Povlishock, J.T., Mountney, A., Browning, M., Deng-Bryant, Y., Yan, H.Q., Jackson, T.C., Catania, M., Glushakova, O., Richieri, S.P., and Tortella, F.C. (2016). Synthesis of findings, current investigations, and future directions: operation brain trauma therapy. J. Neurotrauma 33, 606–614.
43. Eikermann-Haerter, K., Dilekoz, E., Kudo, C., Savitz, S.I., Waeber, C., Baum, M.J., Ferrari, M.D., van den Maagdenberg, A.M., Moskowitz, M.A., and Ayata, C. (2009). Genetic and hormonal factors modulate spreading depression and transient hemiparesis in mouse models of familial hemiplegic migraine type 1. J. Clin. Invest. 119, 99–109.

Address correspondence to:
Nils Henninger, MD, PhD, DrMed
University of Massachusetts Medical School
55 Lake Avenue North
Worcester, MA 01655

E-mail: nils.henninger@umassmed.edu